AIP Applied Physics Letters

Growth of single-crystalline Ru O 2 nanowires with one- and two-nanocontact electrical characterizations

Yee-Lang Liu, Zong-Yi Wu, Kuei-Jiun Lin, Jr-Jeng Huang, Fu-Rong Chen, Ji-Jung Kai, Yong-Han Lin, Wen-Bin Jian, and Juhn-Jong Lin

Citation: Applied Physics Letters **90**, 013105 (2007); doi: 10.1063/1.2428669
View online: http://dx.doi.org/10.1063/1.2428669
View Table of Contents: http://scitation.aip.org/content/aip/journal/apl/90/1?ver=pdfcov
Published by the AIP Publishing

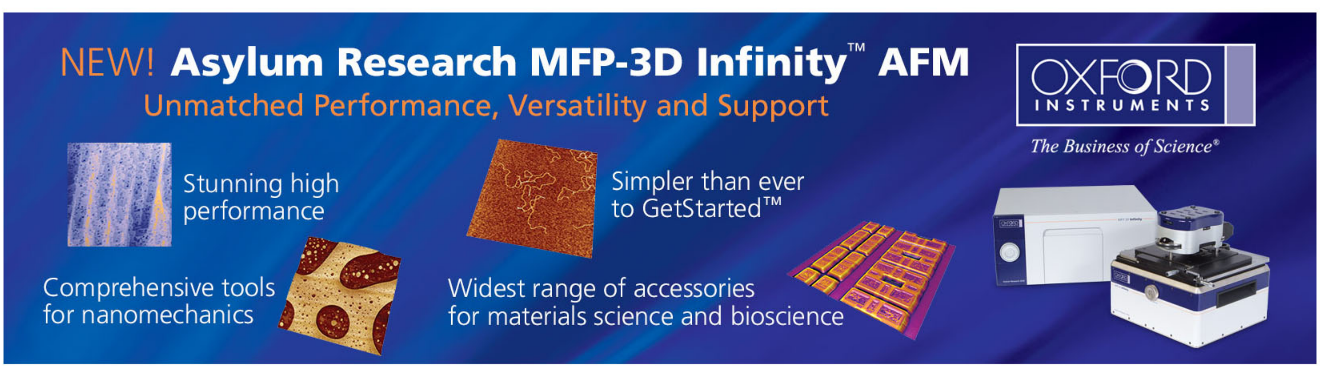

Growth of single-crystalline RuO_2 nanowires with one- and two-nanocontact electrical characterizations

Yee-Lang Liu, Zong-Yi Wu, Kuei-Jiun Lin, Jr-Jeng Huang, Fu-Rong Chen, and Ji-Jung Kai[a),b)]
Center of Electron Microscopy, Department of Engineering and System Science, National Tsing Hua University, Hsinchu 30013, Taiwan

Yong-Han Lin
Institute of Physics, National Chiao Tung University, Hsinchu 30010, Taiwan

Wen-Bin Jian[a),c)]
Department of Electrophysics, National Chiao Tung University, Hsinchu 30010, Taiwan

Juhn-Jong Lin
Institute of Physics, National Chiao Tung University, Hsinchu 30010, Taiwan and Department of Electrophysics, National Chiao Tung University, Hsinchu 30010, Taiwan

(Received 8 September 2006; accepted 2 December 2006; published online 3 January 2007)

Single-crystalline RuO_2 nanowires were grown by using a thermal evaporation method. A control of the sizes (width and length) and the length-to-width ratio of the nanowires were achieved by tuning the growth time. A transmission electron microscope–scanning tunneling microscope technique invoking one-nanocontact electrical characterization was adopted to determine the room-temperature resistivity ($\sim$100 $\mu\Omega$ cm) of the nanowires. An e-beam lithography technique facilitating two-nanocontact measurements was performed to establish the metallic characteristic of individual nanowires. The authors found that a nanocontact may introduce high contact resistance, nonlinear current-voltage characteristics, and even semiconducting behavior in the temperature dependent resistance. [DOI: 10.1063/1.2428669]

The step-edge[1] and e-beam lithography[2,3] techniques, combined with thermal-evaporation deposition, were developed to make one-dimensional metal wires with high length-to-width ratios. Resistances of those top-down fabricated metal wires were measured as functions of temperature and magnetic field, and topics, including weak-localization and electron-electron interaction effects, superconducting-to-normal metal transition, etc., had been investigated.[1,3–6] The crystalline structures of such top-down fabricated metal wires, however, could not be readily determined experimentally. The lately synthesized nanomaterials such as carbon nanotubes,[7] ZnO nanowires (NWs),[8] and other metallic[9,10] and semiconducting[11] NWs were mostly single crystalline according to electron microscopy analysis. Nanoscale electronic devices made of those bottom-up generated, single-crystalline NWs have recently been realized and demonstrated.[12–15]

RuO_2 is an inviting electrical contact material[16] with a room-temperature resistivity of $\sim$35 $\mu\Omega$ cm,[17] which is about twice that of the Ru metal. It crystallizes in the rutile structure[18] and displays good thermal stability up to 600 °C.[19] RuO_2 had been produced into one-dimensional nanorods and NWs by using templates,[10] chemical vapor deposition,[20] reactive sputtering,[21] and other methods.[22] The growth and structural characterization of RuO_2 nanorods had been discussed in the literature[10,20–22] but a control of the length-to-width ratio and of the length and width of the NWs have not been attempted.

Electrical characterizations for the metallic NWs are crucial for their possible applications as interconnects in bottom-up fabricated nanoscale electronic devices, while understanding of the electrical properties of those single-crystalline NWs is mostly lacking. In this letter, we employ a thermal evaporation method to synthesize RuO_2 NWs with controlled sizes. The characterizations of the electrical-transport property of RuO_2 NWs are performed on a two-nanocontact configuration made with the e-beam lithography technique. Alternatively, a transmission electron microscope holder attaching a scanning tunneling microscope probe[23] (TEM-STM) providing a convenient way to obtain the resistance at a specific nanosclae position is adopted for one-nanocontact characterization at room temperature.

RuO_2 NWs were grown in a quartz tube inserted in a furnace. The quartz tube was sealed and evacuated to a base pressure of 10^{-3} torr. A source material of stoichiometric RuO_2 powder (Aldrich, 99.9%) was placed in the center of the quartz tube and heated to 920–960 °C. Oxygen gas (99.9%) was introduced into the quartz tube and the chamber was maintained at a constant pressure of 2 torr. Silicon wafer substrates with gold nanoparticles (Ted-pella, 5–40 nm in diameter) as catalyst predeposited on them were loaded at the downstream end of the quartz tube, where the temperature was kept at 450–670 °C. Several hours later, single-crystalline RuO_2 NWs were grown on the substrates. One-nanocontact electrical characterization was performed on a TEM-STM system with a STM gold tip sharpened by employing focused ion beam. After the formation of a one nanocontact between the gold tip and the single RuO_2 NW, the current-voltage (I-V) behavior and the resistance of the NW could be studied. Two nanocontacts on a single NW were

[a)]Authors to whom correspondence should be addressed.
[b)]Electronic mail: jjkai@ess.nthu.edu.tw
[c)]Electronic mail: wbjian@mail.nctu.edu.tw

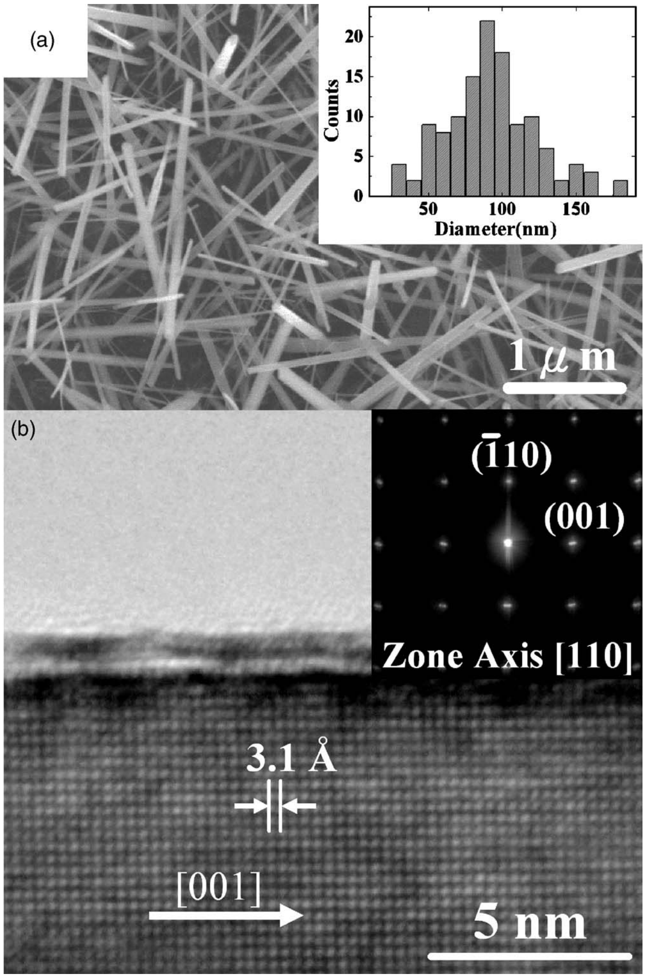

FIG. 1. (a) SEM image of RuO_2 NWs. The inset shows a distribution of the widths of the NWs. (b) High-resolution TEM image of a single-crystalline RuO_2 NW with its corresponding selected-area electron diffraction pattern (inset).

fabricated by the standard e-beam lithography technique with contact electrodes of Cr/Au (~10/90 nm) films. Measurements of temperature dependent resistance were carried out in a ^{4}He dipper, using a Linear Research LR700 resistance bridge operating at an ac current of 30 nA. The linearity of the *I-V* curves was checked before recording the resistance at various temperatures.

A top-view SEM image in Fig. 1(a) shows our RuO_2 NWs. A rectangular cross section, with average length of several micrometer and average width of ~90 nm, was determined. A broad distribution in the width is shown in the inset of Fig. 1(a). The crystalline structure was determined to be the rutile structure with lattice constants $a=b=4.500\pm0.005$ Å and $c=3.101\pm0.006$ Å by using x-ray diffraction. Figure 1(b) displays high-resolution TEM image of a single RuO_2 NW. As indicated, the growth direction is along the [001] direction, being consistent with previous results.[20] The [110] growth direction as reported in Ref. 22 was not found in our samples. The corresponding electron diffraction pattern is shown in the inset of Fig. 1(b). The lattice constant c was estimated in the TEM image to be 3.1 Å.

Gold nanoparticles were used as catalyst in our growth of the NWs. However, we found that a change in the gold nanoparticle diameter from 5 to 40 nm did not lead to appreciable variation in the width of our NWs. The control of the

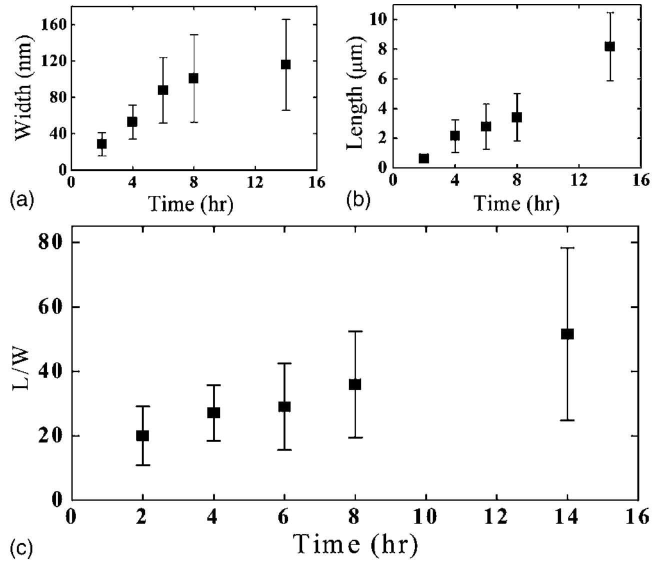

FIG. 2. (a) Average width, (b) average length, and (c) length-to-width ratio of RuO_2 NWs as a function of growth time.

sizes (width and length) of the RuO_2 NWs was achieved by adjusting the growth time. The width, length, and the length-to-width ratio of the NWs as a function of the growth time are displayed in Figs. 2(a)–2(c), respectively. The width of the NWs varies linearly with the growth time initially and saturates after 8 h. The length, length-to-width ratio, and their corresponding standard deviations increase monotonically with the growth time.

A schematic drawing in Fig. 3(a), together with a high resolution TEM image, illustrates the TEM-STM technique for our measurements of the NW resistivity at room temperature. Though the nanocontact resistance is very sensitive to the interfacial structures and the NWs could be differently doped, we assume average contact resistance and NW resistivity in our measurements. Typical *I-V* curves are shown in

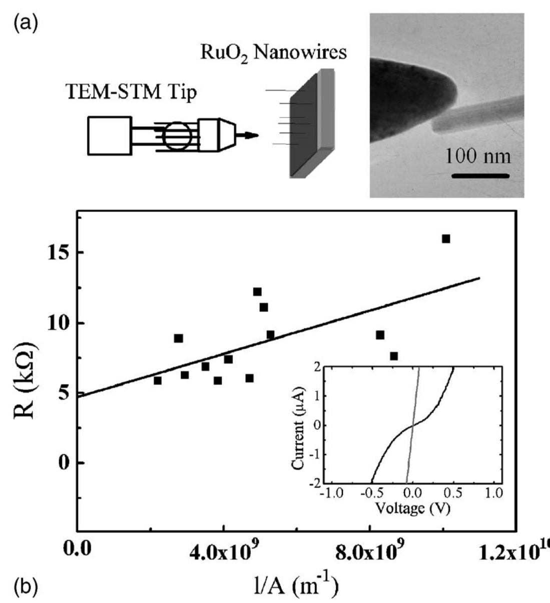

FIG. 3. (a) Schematic illustration of the TEM-STM technique. The TEM image (right) displays a one nanocontact for electrical characterization. (b) TEM-STM measured resistance as a function of l/A of the NWs. The inset displays the *I-V* curves for untreated (nonlinear) and treated (linear) nanocontacts.

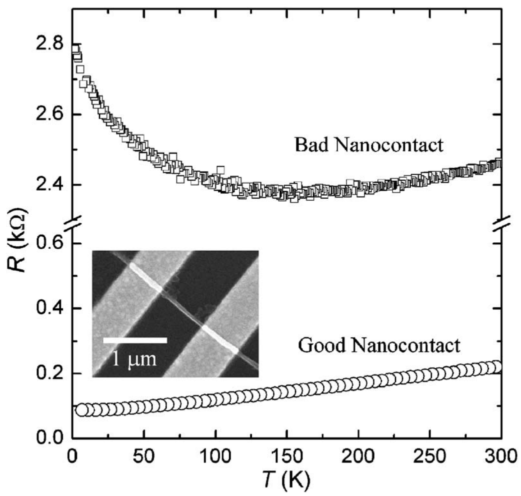

FIG. 4. Two typical temperature dependent resistance curves obtained from two-nanocontact electrical characterizations on single RuO_2 NWs having bad (top) and good (bottom) nanocontacts. The inset shows SEM image of a 70 nm RuO_2 NW with two electrodes.

the inset of Fig. 3(b). Notice that the TEM-STM measurement produced nonlinear *I-V* curves for our untreated nanocontacts. We used the techniques of mechanical indentation, polishing, and focus e-beam annealing to improve the quality of the nanocontact between the NW and the electrode of a STM tip. After these treatments, we obtained linear *I-V* curves obeying the Ohmic law. The resistance R as a function of the ratio of length (l) to cross-sectional area (A) of the NWs was obtained and fitted with the relation $R = R_C + \rho l / A$, where R_C and ρ are the nanocontact resistance and the resistivity of the NW, respectively. A linear least-squares fit indicates $R_c \sim 5$ kΩ and $\rho \sim 100\ \mu\Omega$ cm. The ρ value is about three times of the bulk value.

Temperature dependent resistances measured using a two-nanocontact configuration (the inset) are displayed in Fig. 4. Even though the contact resistance is only on the order of 2–3 kΩ (top curve), the measured resistance already exhibit nonmetallic behavior (at low temperatures) implying bad nanocontacts in this case. In the other case where the resistance is one order smaller (bottom curve), implying good nanocontacts between the NW and the electrodes, the measured resistance demonstrates metallic feature all the way down to liquid-helium temperatures. The resistivity of our NWs was determined to be 100–300 $\mu\Omega$ cm, which is in line with that obtained from our four-point measurements (not shown) and of the same order of magnitude of that obtained from the TEM-STM technique. Based on the TEM-STM and e-beam results, we attribute the bad nanocontact resistance of several kilohms to the conductive rough surface formed between the NW and the electrode.[24] At low temperatures, the rising resistance of the bad nanocontact could be fitted well with the electron hopping theory in granular metals[25] possibly generated in the nanocontact.

In summary, single-crystalline RuO_2 NWs with [001] growth direction have been synthesized by the thermal evaporation method. The sizes of the NWs were controlled by the growth time. The TEM-STM technique provided a handy one-nanocontact measurement of the NW resistance, accompanied with a contact resistance of several kilohms. The metallic feature of the NWs can be verified by the two-nanocontact electrical characterization only when the contact resistance is at least one order of magnitude smaller than that encountered in the one-nanocontact measurement. Metallic RuO_2 NWs may serve as inviting interconnects in nanoelectronics.

This work was supported by the Taiwan National Science Council under Grant Nos. NSC 94-2112-M-009-020, NSC 93-2120-M-009-009, and NSC 94-2120-M-009-010 and by the MOE ATU Program.

[1] N. Giordano, W. Gilson, and D. E. Prober, Phys. Rev. Lett. **43**, 725 (1979).
[2] T. A. Fulton and G. J. Dolan, Appl. Phys. Lett. **42**, 752 (1983).
[3] J. C. Licini, G. J. Dolan, and D. J. Bishop, Phys. Rev. Lett. **54**, 1585 (1985).
[4] J. J. Lin and N. Giordano, Phys. Rev. B **33**, 1519 (1986).
[5] N. Giordano, Phys. Rev. Lett. **61**, 2137 (1988).
[6] J. F. Lin, J. P. Bird, L. Rotkina, and P. A. Bennett, Appl. Phys. Lett. **82**, 802 (2003).
[7] S. Iijima, Nature (London) **354**, 56 (1991).
[8] M. H. Huang, S. Mao, H. Feick, H. Yan, Y. Wu, H. Kind, E. Weber, R. Russo, and P. Yang, Science **292**, 1897 (2001).
[9] Z. Zhang, J. Y. Ying, M. S. Dresselhaus, J. Mater. Res. **13**, 1745 (1998).
[10] B. C. Satishkumar, A. Govindaraj, M. Nath, and C. N. R. Rao, J. Mater. Chem. **10**, 2115 (2000).
[11] A. M. Morales and Charles M. Lieber, Science **279**, 209 (1998).
[12] H. Dai, E. W. Wong, and Charles M. Lieber, Science **272**, 523 (1996).
[13] X. Duan, Y. Huang, Y. Cui, J. Wang and Charles M. Lieber, Nature (London) **409**, 66 (2001).
[14] Y. Cui and Charles M. Lieber, Science **291**, 851 (2001).
[15] H. W. C. Postma, T. Teepen, Z. Yao, M. Grifoni, and C. Dekker, Science **293**, 76 (2001).
[16] R. G. Vadimsky, R. P. Frankenthal, and D. E. Thompson, J. Electrochem. Soc. **126**, 2017 (1979).
[17] W. D. Ryden, A. W. Lawson, and C. C. Sartian, Phys. Rev. B **1**, 1494 (1970).
[18] K. M. Glassford and J. R. Chelikowsky, Phys. Rev. B **47**, 1732 (1993).
[19] M. L. Green, M. E. Gross, L. E. Papa, K. J. Schnoes, and D. Brasen, J. Electrochem. Soc. **132**, 2677 (1985).
[20] C. C. Chen, R. S. Chen, T. Y. Tsai, Y. S. Huang, D. S. Tsai, and K. K. Tiong, J. Phys.: Condens. Matter **16**, 8475 (2004).
[21] K. W. Cheng, Y. T. Lin, C. Y. Chen, C. P. Hsiung, J. Y. Gan, J. W. Yeh, C. H. Hsieh, and L. J. Chou, Appl. Phys. Lett. **88**, 043115 (2006).
[22] C. Ducati, D. H. Dawson, J. R. Saffell, and P. A. Midgley, Appl. Phys. Lett. **85**, 5385 (2004).
[23] M. W. Larsson, L. R. Wallenberg, A. I. Persson, and L. Samuelson, Microsc. Microanal. **10**, 41 (2004).
[24] L. Kogut and K. Komvopoulos, J. Appl. Phys. **94**, 3153 (2003).
[25] B. Abeles, Ping Sheng, M. D. Coutts, and Y. Arie, Adv. Phys. **24**, 407 (1975).